

Supplementary Material A. List of taxa from scientific surveys.

Table A1. List of taxa from scientific surveys, FAO codes from fishing data and trophic groups from (Corrales et al., 2022). The biomass and abundance density statistics are averaged over several years depending of the survey (2014-2018 for LANGOLF and 2013-2016; 2018-2019 for EVHOE). In orange, the species selected for the provisioning ecosystem service analysis. \$: EVHOE and *: LANGOLF.

Market status	FAO code-Name	Production from the GV (2016-2020)		Taxon and survey	Density estimated over the all area		Trophic group
		Landings (tons)	Value (k€)		Abundance (ind/km2)	Biomass (tons/km2)	
First importance market species	CRE-Brown crab	102	281	<i>Cancer pagurus</i> \$	13	12	Benthos feeders decapods
	GUR-Gunards	165	210	<i>Chelidonichthys cuculus</i> \$	214	17	Small demersal fishes
	COE-Conger	406	670	<i>Conger conger</i> \$	47	51	Large demersal fishes
	OCT-Octopus	93	173	<i>Eledone cirrhosa</i> \$	112	16	Benthic cephalopods
	GUR-Gunards	165	210	<i>Eutrigla gurnardus</i> \$	31	5	Small demersal fishes
	ILL-Red squids	81	224	<i>Illex coindetii</i> \$	291	13	Squids
	LEZ-Megrim	627	2,119	<i>Lepidorhombus sp</i> *	1,866	355	Megrim
	SRX-Rays (except R. undulata)	175	421	<i>Leucoraja naevus</i> \$	15	15	Rays and skates
	SQZ-Squids	63	501	<i>Loligo forbesii</i> \$	141	9	Benthic cephalopods
	MNZ-Monkfishes	1,427	6,547	<i>Lophius budegassa</i> \$	30	38	Anglerfish
				<i>Lophius piscatorius</i> \$	22	35	Anglerfish
	WHG-Whiting	212	517	<i>Merlangius merlangus</i> \$	51	15	Medium demersal fishes
				<i>Merluccius merluccius</i> \$	8,583	1,171	
	HKE-Hake	5,009	13,305	<i>Merluccius merluccius (juveniles)</i> \$	8,629	704	Hake juvenile
				<i>Nephrops norvegicus (estimated by burrows)</i> *	196,744	3,812	Norway lobster
	NEP-Norway lobster	2,345	27,655	<i>Nephrops norvegicus</i> *	12,378	240	
	SYC-Spotted sharks	265	130	<i>Scyliorhinus canicula</i> \$	254	108	Demersal sharks
	CTC-Cuttlefishes	130	542	<i>Sepiidae</i> \$	71	4	Benthic cephalopods
	SOL-Common sole	520	6,903	<i>Solea solea</i> \$	11	4	Common sole
SQZ-Squids	63	501	<i>Todaropsis eblanae</i> \$	156	5	Squids	
BIB-Pouts	268	257	<i>Trisopterus luscus</i> \$	286	58	Poor cod	
JOD-John Dory	156	1,812	<i>Zeus faber</i> \$	49	24	Large demersal fishes	

Table A1. Continued.

Market status	FAO code-Name	Production from the GV (2016-2020)		Taxon and survey	Density estimated over the all area		Trophic group	
		Landings (tons)	Value (k€)		Abundance (ind/km2)	Biomass (tons/km2)		
No significant fishing on the area				<i>Alcyonacea</i> *	1,002			
				<i>Alloteuthis</i> \$	12,553	27	Squids	
				<i>Alpheus glaber</i> \$	30	0.05	Benthos feeders decapods	
				<i>Anemone unid</i> *	9,296	49		
				<i>Anseropoda placenta</i> \$	35	0.37	Echinoderms	
				<i>Aphrodita aculeata</i> \$	15	0.35		
				<i>Argentina sphyraena</i> \$	587	9	Other planktivorous fishes	
				<i>Arnoglossus imperialis</i> \$	73	1	Flatfishes	
				<i>Arnoglossus laterna</i> \$	37	0.37	Flatfishes	
				<i>Astropecten irregularis</i> \$	154	1	Echinoderms	
				<i>Callionymus sp</i> *	1,086	53	Small demersal fishes	
				<i>Cepola macrophthalma</i> \$	14	0.67		
				<i>Chlorotocus crassicornis</i> \$	71	0.17	Zooplankton feeding shrimps	
				<i>Crangon allmanni</i> \$	799	1	Benthos feeders decapods	
				<i>Crinoidea</i> *	55,288			
				<i>Dichelopandalus bonnieri</i> \$	65	0.14	Benthos feeders decapods	
				<i>Enchelyopus cimbrius</i> \$	24	0.75		
				<i>Gastropteron rubrum</i> \$	29	0.05		
				<i>Goneplax rhom</i> *	941	6	Detritus feeders decapods	
				<i>Hydrozoa</i> *	159,771	4,851		
				<i>Lesueurigobius friesii</i> \$	217	0.6	Small demersal fishes	
				<i>Liocarcinus depurator</i> \$	322	2	Benthos feeders decapods	
				<i>Liocarcinus holsatus</i> \$	30	0.16	Benthos feeders decapods	
				<i>Macropipus tuberculatus</i> \$	19	0.21	Benthos feeders decapods	
				<i>Macropodia tenuirostris</i> \$	37	0.08	Benthos feeders decapods	
				<i>Maurolicus muelleri</i> \$	23	0.11	Mesopelagic fishes	
		MKG-Thickback sole	1	4	<i>Microchirus variegatus</i> \$	267	8	Flatfishes
					<i>Munida rugosa</i> *	25,403	212	Detritus feeders decapods
				<i>Ophiuroidea</i> *	6,394	35	Echinoderms	
				<i>Paguroidea</i> *	2,442	11	Detritus feeders decapods	
				<i>Pennatulacea</i> *	24,376	488		
	GFB-Greater forkbeard	7	11	<i>Phycis blennoides</i> \$	40	6	Medium demersal fishes	
				<i>Pomatoschistus minutus</i> \$	36	0.09	Small demersal fishes	
				<i>Pontophilus spinosus</i> \$	34	0.06	Benthos feeders decapods	
				<i>Porania (Porania) pulvillus</i> \$	22	0.27	Echinoderms	
				<i>Processa canaliculata</i> \$	72	0.11	Benthos feeders decapods	

Table A1. Continued.

No significant fishing on the area	<i>Scaphander lignarius</i> \$	23	0.26	
	<i>Sepiolidae</i> \$	944	21	Benthic cephalopods
	<i>Solenocera membranacea</i> \$	66	0.17	Benthos feeders decapods
	<i>Spirographis</i> sp *	5,438	98	
	<i>Stichastrella rosea</i> \$	33	0.34	Echinoderms
	<i>Trisopterus minutus</i> \$	12,582	527	Poor cod

Reference

Corrales, X., Preciado, I., Gascuel, D., Lopez de Gamiz-Zearra, A., Hervann, P.-Y., Mugerza, E., et al. (2022). Structure and functioning of the Bay of Biscay ecosystem: A trophic modelling approach. *Estuar Coast Shelf Sci* 264, 107658. doi: 10.1016/j.ecss.2021.107658.

Supplementary Material B. Description of surveys and procedure for predicting taxa's abundances.

This work aims to get an estimation of the abundance density of as much taxa as possible in the Grande Vasière (GV). The results were used to measure several indicators detailed in the Table 1 in the main text. The predicted density was computed for each taxon and year at the cell centroids of a 2.5 km x 2.5 km grid.

1.1 Survey sampling and protocols

We used sampling data from the two scientific surveys covering the benthic and demersal ecosystem of the GV: LANGOLF TV and EVHOE.

LANGOLF-TV is an underwater video survey led by Ifremer and the Comité National des Pêches Maritimes et des Elevages Marins (CNPMM) to assess the Norway lobster stock by burrow counting. The study area is delineated by the GV as it corresponds to the distribution area of this species in the Bay of Biscay. The video allows to sample a great number of other epibenthic species which have been stored in a database over the 2014-2018 time series. The sampling takes place during April (except for 2014 and in 2015 in September and July respectively) and the protocol is well detailed by Mérillet et al. (2018): *"Videos of the seabed were recorded using a camera (Kongsberg OE14-366, 0.48 megapixel) fixed on a sledge dropped onto the seabed and towed behind the Celtic Voyager RV for 10 minutes [...]. The sledge was equipped with CTD and global positioning system devices recording depth and geographic position, as well as two lasers, spaced 0.75 m apart, that delineated the area covered by the camera (calibrated for a consistent spacing of the area filmed). The locations of [...] sampling sites were chosen along a regular square grid of 8.7 × 8.7 km resolution, built [in 2014] from a first point picked randomly inside the limits of the study area [and visited each year]. At each site, a video transect was recorded at an average speed of 0.85 knots"*. Each video is watched during 7 minutes by an observer for counting. We can also mention that because the sledge cannot be safely lowered on hard substrates, transects that were located on such substrates were not performed.

EVHOE is a bottom trawl survey mainly targeting the demersal species between October and November in the Bay of Biscay and the Celtic Sea. The available time series goes from 1997 to 2020 but it is worth noting that the 2017 year is missing due to technical breakdown in the R/V Thalassa. To be consistent with LANGOLF-TV, we selected only the hauls made between 2013 and 2019 in the north of the continental shelf. This selection area was defined by a depth criterion according to the LANGOLF-TV range of depth (between -30 meters and -160 meters) within the following spatial window: 0° - 6°O; 44°N 30' - 48°N (Figure B1).

Each sampling site is randomly chosen among a set of fishing positions stratified according to depth. The number of sampled hauls by stratum is set with a Neyman allocation fitted on the main species of interest. A wild vertical opening bottom trawl fitted with a codend of 20 mm stretched mesh, a 36 m headline and a 47 m ground rope is towed during 30 minutes at a ~3.5 knots speed. The total catch is weighted and sorted by species for counting. Depending of the species and the total weight catch, a subsample is put aside for length measurements, maturity stage identification and sexing (ageing is made on a new subsample).

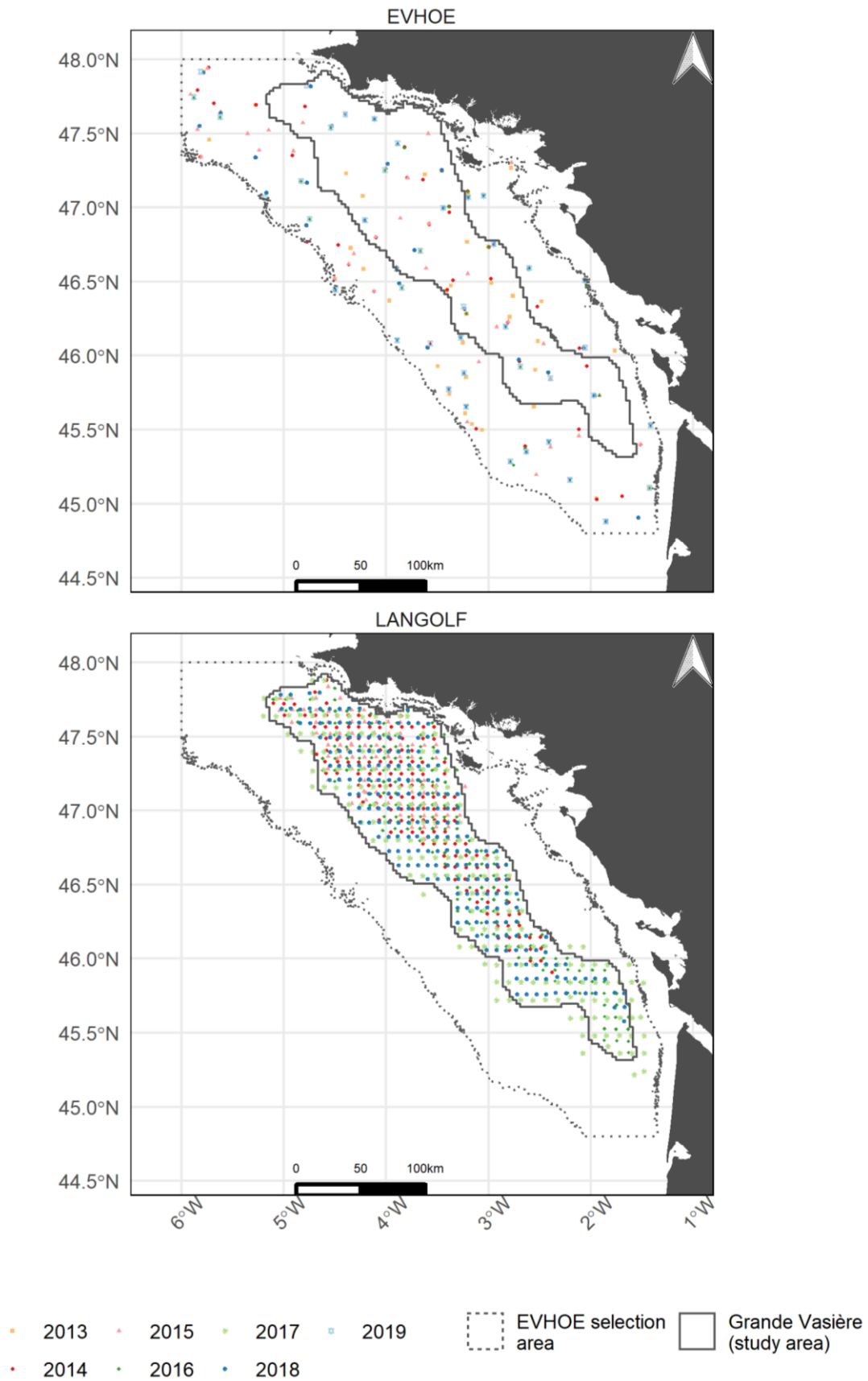


Figure B1. Maps of sampling sites of the LANGOLF TV and EVHOE surveys.

For the sake of simplicity, transects (LANGOLF-TV) and hauls (EVHOE) are called hereafter “station”.

The two surveys differ greatly in their selectivity and swept area by station (Table B1). The LANGOLF-TV counting covers small areas and is exhaustive for a large part of the epibenthic fauna, whereas EVHOE covers larger areas, catching a larger diversity of benthic and demersal species but sometimes with a low catchability.

Table B1. Number of stations (hauls/transects), mean swept area in square meters and number of taxa observed at least one time in the LANGOLF TV and EVHOE surveys.

Survey	EVHOE	LANGOLF-TV
Years sampled	2013-2016 and 218-2019	2014-2018
Nb of stations	269	860
Mean distance between station (km)	42	18
Mean swept area (m²)	64.187 (±8%)	158 (±29%)
Number of taxa	716	41

1.2 Taxa selection

We selected taxa following two criteria:

- 1) Taxon observed on at least 30 stations over the whole time series to get enough points of presence for models fitting;
- 2) Taxon observed at least once during more than the half of the time series to evict as much as possible species subject to “false zeros” (e.g. a species always present but observed one year due to specific conditions of selectivity).

We kept four taxa which do not meet the criterion of the 30 points, but which are important for fishing activities (*Leucoraja naevus*: 27 points) or for biodiversity and bioturbation (*Anseropoda placenta*: 28 points, *Macropipus tuberculatus*: 29 points, *Porania pulvillus*: 28 points). Then, we dropped some taxa from LANGOLF-TV due to their high level of taxonomic aggregation or because they are well identified at the species level in the EVHOE dataset: *Actinopterygii*, Anguilliformes, Jellyfish, Flat fishes, Crabs, *Crustacea*, Shrimps, Sea star, Gadiform, Macrophyte. We also removed two taxa from EVHOE which are badly caught by bottom trawl (*Hyalinoecia tubicola*, *Scalpellum scalpellum*) and one known to be highly mobile and migratory (*Dicentrarchus labrax*). Finally, we had to choose between the two surveys in the case of taxa observed in both (Table B2). We prioritized the LANGOLF-TV survey unless we considered the selectivity of EVHOE to be much greater.

At the end of the process, we kept fourteen taxa from LANGOLF-TV and forty-nine taxa from EVHOE.

Table B2. Duplicated taxa between EVHOE and LANGOLF-TV and the selected survey.

LANGOLF-TV taxa	EVHOE taxa	Selected survey
<i>Actiniaria</i>	<i>Actiniaria ; Adamsia palliata</i>	
<i>Goneplax rhomboides</i>	<i>Goneplax rhomboides</i>	
<i>Callionymus spp</i>	<i>Callionymus lyra ; Callionymus maculatus</i>	
<i>Lepidorhombus spp</i>	<i>Lepidorhombus whiffiagonis</i>	
<i>Crinoidea</i>	<i>Leptometra celtica</i>	
<i>Hydrozoa</i>	<i>Lytocarpia myriophyllum</i>	LANGOLF-TV
<i>Microchirus var</i>	<i>Microchirus variegatus</i>	
<i>Munida rugosa</i>	<i>Munida rugosa</i>	
<i>Nephrops norvegicus</i>	<i>Nephrops norvegicus</i>	
<i>Ophiuroidea</i>	<i>Ophiura ophiura</i>	
<i>Paguroidea</i>	<i>Pagurus prideaux</i>	
<i>Soleidae</i>	<i>Solea solea</i>	
<i>Triglidae</i>	<i>Eutrigla gurnardus ; Chelidonichthys cuculus</i>	
<i>Scyliorhinus spp</i>	<i>Scyliorhinus canicula</i>	EVHOE
<i>Sepiidae</i>	<i>Sepiidae</i>	
<i>Octopus spp</i>	<i>Eledone cirrhosa</i>	

1.3 Spatialized Generalized Linear Models and Kriging procedure

We tested two modelling techniques to predict the density of each taxon and year in each grid cell:

- 1) Generalized Linear Models (GLM) with environmental and anthropogenic predictors and spatial covariance (GLMM);
- 2) Ordinary kriging with an external drift on years, assuming that at the scale of the GV, recruitment dynamic involved much more important temporal variability than at the spatial dimension.

1.3.1 Selection of predictors and transformations

We computed fishing effort from bottom trawls and gillnets and the annual amount of effort versus the month before the survey. It allowed us to disentangle the effect of fishing pressure depending on the species and the temporal scale. We also added several environmental predictors: temperature, speed, roughness, sediment type and depth from data described in Supplementary Material C. Due to seasonal effect of temperature, we considered the annual average and the month average before the survey. Finally, we included a year effect to consider potential recruitment effects over years.

As fishing efforts predictors, roughness and speed showed very skewed distributions, we log-transformed to ensure a linear relationship with the taxa densities. We tested a three degrees orthogonal polynomial transformation over depth and temperature to test for species *preferendum*.

However, we faced to temperature values out of the sample range leading to spurious predictions. Consequently, we left the polynomial transformation on temperature.

1.3.2 Abundance estimation procedure

We compared the GLM and the ordinary kriging results following the methodological procedure detailed in the Figure B2.

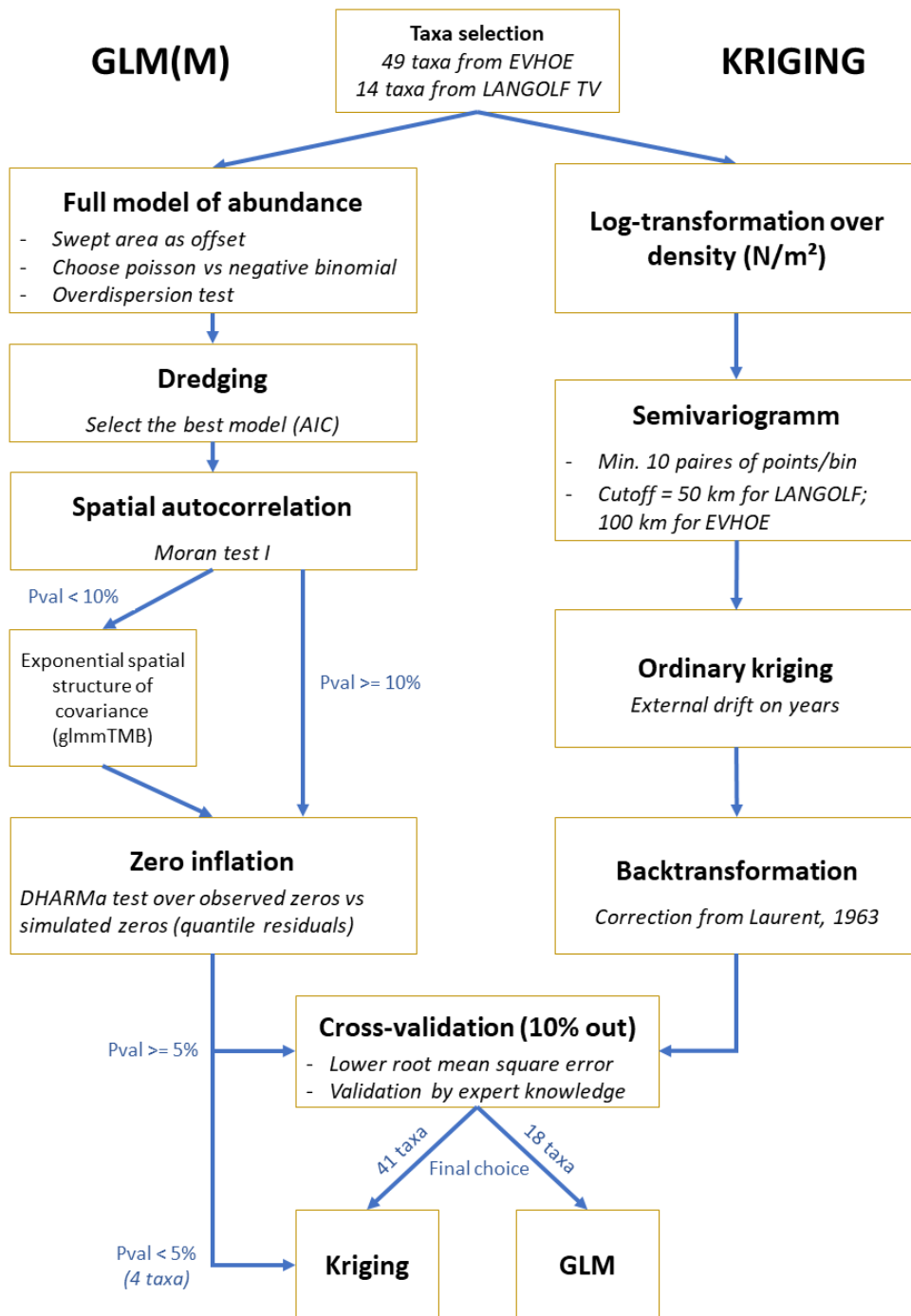


Figure B2. Abundance estimation procedure by taxon from LANGOLF TV and EVHOE surveys data.

GLM procedure

We used the ‘glmmTMB’ R package (Brooks et al., 2017) which allows to fit GLMs with a covariance structure and a negative binomial distribution. The covariance structure takes the form of correlated multivariate gaussian terms treated as random effects. Random effects are fitted by location and the correlation between random effects is exponentially decreasing with distance. Despite their availability in glmmTMB, the gaussian and Matern covariance functions caused convergence troubles and were not included.

We checked the overdispersion of the full model with a Poisson distribution by testing if the dispersion ratio (variance/mean) was higher than one (“check_overdispersion” function from the ‘performance’ R package (Lüdecke et al., 2021; based on the code of Gelman and Hill, 2006). If some overdispersion was detected, we switched to a negative binomial distribution.

Then, we selected the best model according to the AIC criterion through a dredging procedure performed with the “dredge” function from the ‘MuMIn’ R package (Bartoń, 2022). The dredging method allows to test all the combinations of predictors in an efficient way. The annual and monthly bottom trawling fishing time were highly correlated for EVHOE ($\rho_{pearson} = 0.8$). We decided to keep the two predictors, but we did not associate them during the dredging.

We used the DHARMA R package (Hartig, 2022) to compute quantile residuals of the best model and test for zero-inflation and autocorrelation. For each observation, quantile residuals simulate a set of new responses and the associate empirical density function, according to the fitted model and its underpinning hypothesis (e.g. distribution and random effects). Then, the quantile residual is calculated as “the value of the empirical density function at the value of the observed data [...] so a residual of 0 means that all simulated values are larger than the observed value, and a residual of 0.5 means half of the simulated values are larger than the observed value.” (Hartig, 2022).

We looked for spatial autocorrelation with the Moran I test and we raised the p-value threshold of type I error to 10% in order to widely test spatial covariance structure. Indeed, the visual inspection of the quantile residuals map revealed potential local autocorrelation with p-value between 5 and 8%. We chose to test the spatial GLMM for those cases. In one case, overfitting occurred due to a high number of predictors combined to all the random effects of the covariance structure. In this case we got back to the previous step, pick the second-best model and so on until a model can be fitted.

Kriging procedure

We performed universal kriging with external drift on years over the log-transformed density of each taxon, using the ‘gstat’ R package (Pebesma, 2004). We added a constant to the density before the log-transformation to deal with the zero values as described by the eq. (1).

$$LD_i = \log\left(\frac{A_i}{S_i} + \frac{1}{\bar{S}}\right) = \log\left(A_i \frac{\bar{S}}{S_i} + 1\right) \quad (1)$$

With i the station; LD the log-density; A the abundance; S the swept area; \bar{S} the mean swept area over all i .

The back-transformation of log-density after kriging is biased so we need to add a correction term (eq. 2) presented by Laurent (1963) and applied to the kriging by Journel (1980).

$$N_{pred_c} = \exp\left[\widehat{LD}_c + 0.5 \times \sigma_{K_c}^2\right] - 1 \times \frac{P_c}{\bar{S}} \quad (2)$$

With c the grid-cell, N_{pred} the number of individuals predicted at the grid-cell centroid, σ_K^2 the kriging variance, P the grid cell area (6.25 km²).

Final model selection

For a given taxon, we selected the modelling approaches with the best predictive performance. The prediction error was measured by the Predicted Root Mean Square Error estimated by a “leave-10%-out” Monte Carlo cross-validation procedure with 200 iterations.

In case of zero inflation of the final GLM, we kept only the kriging outputs. At the end of the process, 45 distributions of taxa were estimated by kriging and 18 by GLM.

Table B3. Survey, taxon, final model selected, GLM model formula if selected, Zero-inflation detection, ratio between Root Mean Squared Error (RMSE) between GLM and kriging, comments if any deviation from the selection procedure is made.

	Taxon	Final selection	ZI	RMSE ratio GLM/Kriging	Comments
EVHOE	<i>Alloteuthis</i>	KRIGING	YES		
	<i>Alpheus glaber</i>	KRIGING	NO	1.07	
	<i>Anseropoda placenta</i>	GLM	NO	0.93	
	<i>Aphrodita aculeata</i>	KRIGING	NO	1.02	
	<i>Argentina sphyraena</i>	KRIGING	YES	0.93	
	<i>Arnoglossus imperialis</i>	KRIGING	NO	1.01	
	<i>Arnoglossus laterna</i>	KRIGING	NO	1.27	
	<i>Astropecten irregularis</i>	GLM	NO	0.92	
	<i>Cancer pagurus</i>	GLM	NO	1.02	Very flat semi-variogram and tiny difference between the two MSE. Expert selection of the GLM.
	<i>Cepola macrophthalma</i>	KRIGING	NO	1.06	
	<i>Chelidonichthys cuculus</i>	KRIGING	NO	1.03	
	<i>Chlorotocus crassicornis</i>	KRIGING	NO	1.05	
	<i>Conger conger</i>	KRIGING	NO	1.04	
	<i>Crangon allmanni</i>	KRIGING	NO	3.83	
	<i>Dichelopandalus bonnieri</i>	KRIGING	NO	1.08	
	<i>Eledone cirrhosa</i>	KRIGING	NO	1.12	
	<i>Enchelyopus cimbrius</i>	KRIGING	YES		
	<i>Eutrigla gurnardus</i>	GLM	NO	1.00	
	<i>Gastropteron rubrum</i>	GLM	NO	0.94	
	<i>Illex coindetii</i>	KRIGING	NO	1.03	
	<i>Lesueurigobius friesii</i>	KRIGING	NO	11.64	
	<i>Leucoraja naevus</i>	KRIGING	NO	1.18	
	<i>Liocarcinus depurator</i>	KRIGING	NO	1.12	
	<i>Liocarcinus holsatus</i>	KRIGING	NO	1.72	
	<i>Loligo forbesii</i>	KRIGING	NO	1.02	
	<i>Lophius budegassa</i>	KRIGING	NO	1.07	
	<i>Lophius piscatorius</i>	GLM	NO	0.86	
	<i>Macropipus tuberculatus</i>	KRIGING	NO	1.59	
	<i>Macropodia tenuirostris</i>	GLM	NO	1.00	
	<i>Maurollicus muelleri</i>	KRIGING	NO	3.63	
	<i>Merlangius merlangus</i>	KRIGING	NO	3.35	
	<i>Merluccius merluccius</i>	GLM	NO	1.07	The kriging standard error is high on the north-west part of the core distribution whereas the GLM indicates the opposite. In absence of sampling in this area and considering the reasonable difference of MSE we prefer to keep the GLM which is based on habitat prediction.
	<i>Microchirus variegatus</i>	KRIGING	NO	1.02	
	<i>Phycis blennoides</i>	GLM	NO	0.86	
	<i>Pomatoschistus minutus</i>	KRIGING	NO	13.68	
	<i>Pontophilus spinosus</i>	KRIGING	NO	1.00	Almost the same value of RMSE whereas the map of GLM is highly concentrated contrary to the sampling. Kriging is selected.
<i>Porania (Porania) pulvillus</i>	KRIGING	NO	1.07		
<i>Processa canaliculata</i>	KRIGING	NO	1.14		
<i>Scaphander lignarius</i>	GLM	NO	0.95		
<i>Scyliorhinus canicula</i>	GLM	NO	0.97		
<i>Sepiidae</i>	KRIGING	NO	1.00		
<i>Sepiolidae</i>	GLM	NO	0.98		
<i>Solea solea</i>	GLM	NO	0.96		
<i>Solenocera membranacea</i>	KRIGING	NO	1.26		
<i>Stichastrella rosea</i>	KRIGING	NO		Overfitting, kriging is selected.	
<i>Todaropsis eblanae</i>	GLM	NO	0.96		
<i>Trisopterus luscus</i>	KRIGING	NO	1.03		
<i>Trisopterus minutus</i>	KRIGING	YES			
<i>Zeus faber</i>	GLM	NO	0.67		

Table B3. Continued.

	Taxon	Final Selection	ZI	RMSE ratio GLM/Kriging	Comments
LANGOLF TV	<i>Alcyonacea</i>	KRIGING	NO	2.42	
	<i>Anemone unid</i>	KRIGING	NO	1.00	
	<i>Callionymus sp</i>	KRIGING	NO	1.00	
	<i>Crinoidea</i>	KRIGING	NO	1.00	
	<i>Goneplax rhom</i>	GLM	NO	1.00	
	<i>Hydrozoa</i>	KRIGING	NO	1.00	
	<i>Lepidorhombus sp</i>	KRIGING	NO	1.01	
	<i>Munida rugosa</i>	KRIGING	NO	1.10	
	<i>Nephrops norvegicus</i>	GLM	NO	0.98	
	<i>Nephrops norvegicus burrows</i>	GLM	NO	0.73	
	<i>Ophiuroidae</i>	KRIGING	NO	1.12	
	<i>Paguroidea</i>	KRIGING	NO	1.31	
	<i>Pennatulacea</i>	KRIGING	NO	1.05	
	<i>Spirographis sp</i>	KRIGING	NO	1.02	

References

- Bartoń, K. (2022). MuMIn: Multi-model inference. R package version 1.47.1. <<https://CRAN.R-project.org/package=MuMIn>>
- Brooks, M. E., Kristensen, K., van Benthem, K. J., Magnusson, A., Casper, W., Berg, A. N., Skaug, H. J., Mächler, M., and Bolker, B. M (2017). glmmTMB Balances Speed and Flexibility Among Packages for Zero-inflated Generalized Linear Mixed Modeling. *The R Journal* 9:378. <https://doi.org/10.32614/RJ-2017-066>
- Gelman, A., and Hill, J. (2006). *Data Analysis Using Regression and Multilevel/Hierarchical Models*. Cambridge University Press
- Hartig, F. (2022). DHARMA: Residual Diagnostics for Hierarchical (Multi-Level / Mixed) Regression Models. R package version 0.4.6. <<https://CRAN.R-project.org/package=DHARMA>>
- Journel, A. G. (1980). The lognormal approach to predicting local distributions of selective mining unit grades. *Mathematical Geology* 12:285–303. <https://doi.org/10.1007/BF01029417>
- Laurent, A. G. (1963). Conditional distribution of order statistics and distribution of the reduced i th order statistic of the exponential model. *Annals of Mathematical Statistics* 34:652-657.
- Lüdecke, D., Ben-Shachar, M. S., Patil, I., Waggoner, P., and Makowski, D. (2021). performance: An R Package for Assessment, Comparison and Testing of Statistical Models. *Journal of Open Source Software* 6:3139. <https://doi.org/10.21105/joss.03139>
- Mérillet, L., Robert, M., Salaün M., Schuck, L., Mouchet, M., and Kopp, D. (2018). Underwater video offers new insights into community structure in the Grande Vasière (Bay of Biscay). *Journal of Sea Research* 139:1–9. <https://doi.org/10.1016/j.seares.2018.05.010>
- Pebesma, E. J. (2004). Multivariable geostatistics in S: the gstat package. *Computers and Geosciences* 30:683–691. <https://doi.org/10.1016/j.cageo.2004.03.012>

Supplementary Material C. Description of fishing and environmental data.

Table C1. Description and source of the data used. Dependent indicators in italic mean that the data was used indirectly as a predictor in the species distribution models.

Description	Spatial resolution or format	Available period	Variables of interest	Reference/Source	Dependent indicators
VMS data crossed with fishing sales' notes and logbook data provided by the French National administration and processed by Ifremer (SACROIS algorithm). Available at the gear and year levels for vessels of total length ≥ 12 meters.	Grid (0.05° x 0.05°)	2016-2020	Landing quantity (kg); landing value (euros); Fishing time (hours)	French Directorate of Marine Fisheries and Aquaculture (DGAMPA), SIH (2017)	Fishing effort , <i>P.1.1, P.1.2, R.1.1, R.1.2, R.2.1, R.2.2, R.3.1</i>
Sampling data by taxon and year from the bottom trawl survey EVHOE in the Bay of Biscay and Celtic Sea. For some species, the length distribution is available.	Haul location	2013-2019 (2017 is missing due to broken engine)	Number of individuals; Biomass (kg)	Data from Ifremer's fisheries monitoring campaigns- SIH - https://sih.ifremer.fr/Ecosystemes/Donnees-de-campagnes	P.1.1, P.1.2, R.1.1, R.1.2, R.2.1, R.2.2, R.3.1
Sampling data from the LANGOLF-TV survey in the Grande Vasière (underwater video to assess Norway lobster burrows and benthic communities).	Transect location	2014-2018	Number of individuals	Ifremer/Comité Nationale des Pêches Maritimes et des Elevages Marins	
Marine sediments areas of prospection in metropolitan France.	Polygons		Inclusion/exclusion of the areas	Simplet (2020)	MS prospection
Biomass index from fishing data of recruited individuals of <i>Solea solea</i> by year and month in the Bay of Biscay.	Grid (0.05° x 0.05°)	2008-2018	Biomass index	Alglave et al. (2022)	R.3.2
Monthly averaged bottom current speed, bottom temperature and bottom salinity from the MARS 3D hydrodynamic model	Grid (2.5 x 2.5 km)	2012-2019	Bottom current speed and bottom temperature	Lazure and Dumas (2008)	<i>P.1.1, P.1.2, R.1.1, R.1.2, R.2.1, R.2.2, R.3.1</i>
World map of marine sediments	Polygons		Sediment type	Garlan et al. (2018)	<i>P.1.1, P.1.2, R.1.1, R.1.2, R.2.1, R.2.2, R.2.3, R.3.1</i>
Bathymetry	Grid (~75m x 115m)		Depth	EMODnet Bathymetry Consortium (2018)	<i>P.1.1, P.1.2, R.1.1, R.1.2, R.2.1, R.2.2, R.3.1</i>
Experimental floating offshore windfarms between Groix (France) and Belle-île (France)	Polygons		Inclusion/exclusion of the areas	www.geocatalogue.fr/Detail.do?fileIdentifiant=a00c44c2-4965-48a4-9c6e-2cd586bc7e80	FOW
Future floating offshore windfarms area in south Brittany (France)	Polygons		Inclusion/exclusion of the area	JORF n° 0117, 2021	FOW

References

- Alglave, B., Rivot, E., Etienne, M. P., Woillez, M., Thorson, J. T., and Vermard, Y. (2022). Combining scientific survey and commercial catch data to map fish distribution. *ICES Journal of Marine Science* 79:1133-1149. <https://doi.org/10.1093/icesjms/fsac032>
- EMODnet Bathymetry Consortium EMODnet Digital Bathymetry (DTM) (2018). In: Sextant. <https://sextant.ifremer.fr/geonetwork/srv/api/records/18ff0d48-b203-4a65-94a9-5fd8b0ec35f6>.
- Garlan, T., Gabelotaud, I., Lucas, S., & Marchès, E. (2018). A World Map of Seabed Sediment Based on 50 Years of Knowledge. *World Academy of Science, Engineering and Technology, International Journal of Computer and Information Engineering*, 5.
- JORF n° 0117 (2021). Décision du 18 mai 2021 consécutive au débat public portant sur les projets d'éoliennes flottantes au sud de la Bretagne et leur raccordement
- Lazure, P., and Dumas, F. (2008). An External-Internal Mode Coupling for a 3D Hydrodynamical Model for Applications at Regional Scale (MARS). *Advances in Water Resources* 31:233–250. <https://doi.org/10.1016/j.advwatres.2007.06.010>
- Système d'Information Halieutique (SIH) (2017). Données de production et d'effort de pêche (SACROIS) – 2003-2017. Ifremer SIH. Available at: <http://doi.org/10.12770/3e177f76-96b0-42e2-8007-62210767dc07>
- Simplet, L. (2020) Données extraction de granulats (titres miniers et autorisations de travaux). In: Données extraction de granulats (titres miniers et autorisations de travaux). <https://sextant.ifremer.fr/Donnees/Catalogue>.

Supplementary Material D. Particle size from the World Map of Seabed Sediment and associate scoring for carbon storage.

Table D1. Description of each sediment type available in the World Map of Seabed Sediment from Garlan et al. (2018) and associate carbon storage efficiency score.

Sediment type	Description	Carbon storage efficiency score
Rocks	Rocks	0
Little rocks	Sediment with 50-100% of detritus particles > 20 mm	0
Sand & little rocks	Sediment with little rocks and 15-50% of gravels	1
Gravels	Sediment with 50-100% of particles between 2 and 20 mm	2
Gravels & Sand	Sediment with gravels and 15-50% of sand	2.5
Sand & Gravels	Sediment with sand and 15-50% of gravels	3
Sand	Sediment with 50-100% of particles between 0.5 and 2 mm	4
Muddy sand	Sediment with sand and 5-20% of particles between 0.05 and 0.5 mm	4.5
Fine sand	Sediment with 50-100% of particles between 0.05 and 0.5 mm	5
Fine muddy sand	Sediment with fine sand and 5-20% of particles < 0.5 mm	5.5
Sandy mud	Sediment with mud and 5-20% of particles between 0.5 and 2 mm	6
Silt	Sediment with 50-100% of particles between 0.01 and 0.05 mm	6
Mud	Mix with silt and clay	7

Reference

Garlan, T., Gabelotaud, I., Lucas, S., & Marchès, E. (2018). A World Map of Seabed Sediment Based on 50 Years of Knowledge. *World Academy of Science, Engineering and Technology, International Journal of Computer and Information Engineering*, 5.

Supplementary Material E. Ecosystem services

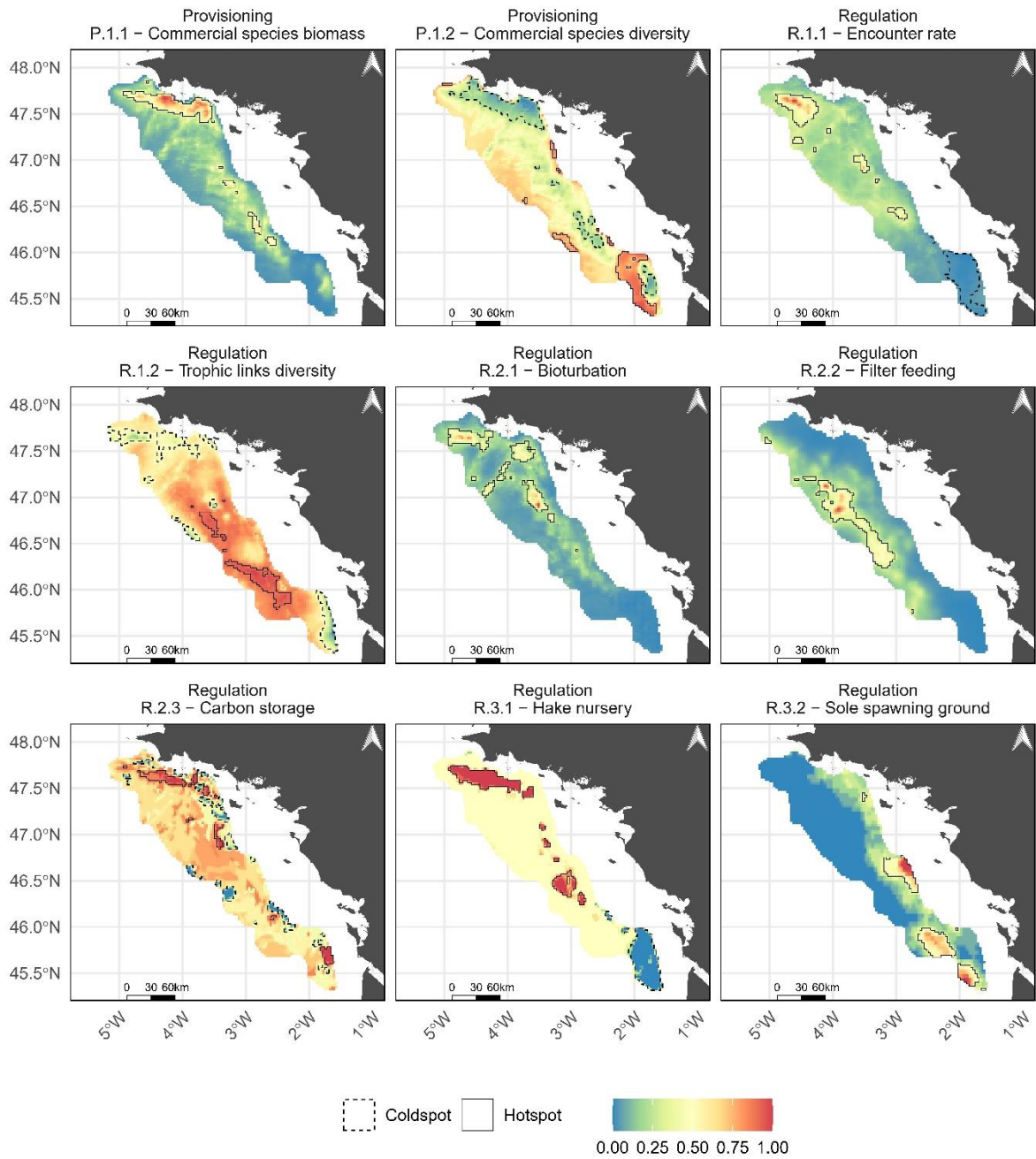


Figure E1. Individual maps of EPs indicators as defined in the Table 1 of the main text. All values are standardized between 0 (no supply) and 1 (maximum supply).

Table E1. Unit, mean, median, minimum and maximum values for each EP indicator over the 3373 grid cells of the GV.

Ecosystem Process	Unit	Mean	Median	Min	Max
P.1.1 Commercial species biomass	Kilograms	36 799	27 907	2 689	189 813
P.1.2 Commercial species diversity		0.46	0.45	0.09	0.85
R.1.1 Encounter rate	No dimension [0; 1]	2.88E-09	2.75E-09	5.90E-10	1.28E-08
R.1.2 Trophic links diversity		0.81	0.81	0.62	0.89
R.2.1 Bioturbation	No dimension [0; max(BPC)]	20.90	16.13	4.53	131.56
R.2.2 Filter feeding	Number of individuals	1 628 416	1 267 508	186 854	10 170 349
R.2.3 Carbon storage	Scoring [0; 7]	4.42	4.50	0	7.00
R.3.1 Hake nursery		0.02	0.00	-1.00	1.00
R.3.2 Sole spawning ground	NPI [-1; 1]	0.14	0.01	0.00	1.00